XLI CILAMCE
XLI Ibero-Latin American Congress on Computational Methods in Engineering
16-19 November, 2020 FOZ DO IGUAÇU PARANÁ - BRAZIL

A Parametric Study of Breaking and Coalescence Mechanisms: Qualitative Analysis of Surface Tension Influence via Computational Simulation of Two-Phase Flow in an Upward Bubble Column.

Vinicius Pacheco Franco[1], Norminda Luiza Oliveira Bodart[1], Vitor Pancieri Pinheiro[1,2], Lucca Dalvi Vargas Melo[1], Larissa Maciel de Almeida[1],

[1]*Programa de Iniciação Científica - Pró-Reitoria de Pesquisa, Pós-Graduação e Extensão - PRPPGE, Universidade Vila Velha*
ES, Brasil
[2]*Programa de Pós-Graduação em Engenharia Mecânica - PPGEM, Universidade Federal do Espírito Santo*
ES, Brasil
vitor.pinheiro1987@gmail.com

Abstract. The vast applicability of the gas-liquid multiphase flow in bubble columns within the engineering fields related to the biochemical, oil and gas, as well as the steel industry, it makes for a compelling research subject. This paper focuses on analyzing the quantitative influence of the surface tension over bubble breaking and coalescence mechanisms using VOF multiphase flow and RANS SST $\kappa - \omega$ to treat the turbulence related features. The simulations were performed by ANSYS Fluent fluid dynamics tool and they exhibit good agreement when properly validated using the axial velocity profile in comparison to other numerical simulations and experimental data available in the literature. Moreover, the results reveal an interesting behavior of the diperse phase as the surface tension was gradually descreased: the disperse phase's inertia is reduced while the bubble breaking mechanism gets more intense. In view of the results regarding the topology, it allows for a broader investigation of the impact of different parameters on the interaction of the phase dynamics, in particular breaking and coalescence processes.

Keywords: Bubble Columns; Computational Fluid Dynamics; Breaking and Coalescence Mechanisms; Surface Tension.

1 Introduction

The behavior and dynamics of fluid interfaces in a multiphase system constitute an issue of substantial importance, given its vast applicability in countless industrial processes, namely, in the chemical and petrochemical industry [1]. The multiphase flow is comprised by interfaces between the multiple phases, where the properties become discontinuous which subsequently poses a challenge to predicting the dynamics of the flow [2]. In the same regard, the upward bubble column constitutes a complex issue to the use of empirical methods. Considering the intricate nature of the experimental conditions [3], numerical solutions are ultimately a more feasible approach [4],[5].

In the context of the mathematical modelling of multiphase flow, the challenges involved in the process are both abundant and fascinating, such as the choice of an appropriate media process [1], surface tracking equations [6], modelling of forces [7],[8] among many others. The selection of a fitting multiphase model to describe the behavior of the phases, it is a core demand and it can be achieved through two different approaches: Eulerian and Lagrangian; as for instance, the two-fluid model, mixture models, disperse particle model, volume of fluid [6],[9],[10]. The choice of these models for numerical simulations is a function of, among other factors, the expected topology between phases, rheology and thermophysical properties of the fluid, the required level of interfacial detailing and the type of coupling between phases.

In addition to the barriers imposed by the special interchange of the phases, which is innate to multiphase flow, there is also the frequent presence of turbulent phenomena that demand specific treatment. The turbulent modelling can be addressed in general terms by three approaches: direct numerical simulation [11], large eddy simulation (LES) [12] or by models which are based on averaged equations of Navier-Stokes (RANS) [13]. The first two options demand plenty of computational resources, while RANS is a more accessible option as it demands

less computational efforts, which explains its diffusion in research [14].

The present paper aims to numerically solve an upward air-water bubble column using *Fluent Ansys'* CFD tool, which allows for a qualitative view of the dispersed phase topology. Regarding the multiphase modelling, the volume of fluid method (VOF), proposed by Hirt and Nichols [9], was chosen given its capability to track well defined interfaces and accurately describe them. As for the turbulence modelling, the RANS SST $\kappa - \omega$ was selected given its satisfactory performance in previous research with similar geometries [15]. As a preliminary study, various transient numerical simulations were performed by varying the time frame and surface tension magnitude, in order to understand the influence of surface tension over breaking and coalescence mechanisms.

2 Mathematical Model

According to the principles of continuum mechanics, the hydrodynamic description of the flow of a Newtonian fluid makes use the of continuity and momentum conservation equations [16] [17]. Given the presence of two or more phases that interact in the flow, it implicates in the remodelling of the equations in order to better represent these interactions. Hence, a few approaches such as the mixture model, two-fluid and volume of fluid models were created to mathematically describe the multiphase flow [1].

A widely used model is the volume of fluid model, which is based on a Eulerian approach towards the treatment of the phases. An interesting aspect of this model is the sharing of the velocity field, which allows for the solution of the problem while employing less computational effort, since it utilizes only one equation of mass and momentum conservation, represented by the expressions 1 and 2, which can be seen in [18].

$$\frac{\partial \rho_m}{\partial t} + \nabla \cdot (\rho_m \overrightarrow{u_m}) = S \tag{1}$$

$$\frac{\partial}{\partial t}(\rho_m \overrightarrow{u_m}) + \nabla.(\rho_m \overrightarrow{u_m}\overrightarrow{u_m}) = -\nabla P + \rho_m \overrightarrow{g} + \nabla\left[\mu_m\left(\nabla \overrightarrow{u_m} + \nabla \overrightarrow{u_m}^T\right)\right] + \overrightarrow{T}_\sigma \tag{2}$$

Where ρ symbolizes the specific mass, u and v the velocity field, P the pressure field, S the net mass balance, μ viscosity, T surface tension force and lastly g represents gravity. Besides applying the principles of mass and momentum conservation, a new differential expression 3 is added, in an effort to obtain a volumetric fraction of the phases in each volume in a fluid domain. It's possible to observe a strong resemblance to the equation of continuity, since it possesses the same mathematical structure in conserving the phase on the volume of control and determining where the interface is placed [19].

$$\frac{\partial}{\partial t}\left(\alpha_q \rho_q\right) + \nabla.\left(\alpha_q \rho_q \overrightarrow{v_q}\right) = S_{\alpha_q} + \sum_{p=1}^{n}(\dot{m}_{pq} - \dot{m}_{qp}) \tag{3}$$

Where α represents the volumetric fraction, $\dot{m}$ the mass flow rate. Upon further inspection of equations 1 and 2, it reveals a sub-index m, which is connected to the balance between the properties of the phases in each volume, which in turn can be calculated by equations 4 with the assumptions displayed by the expression 5.

$$\rho_m = \sum_{q=1}^{n}\alpha_q \rho_q \qquad \mu_m = \sum_{q=1}^{n}\alpha_q \mu_q \qquad \overrightarrow{u_m} = \frac{1}{\rho_m}\sum_{q=1}^{n}\alpha_q \beta_q \overrightarrow{u_q} \tag{4}$$

$$0 < \alpha_q < 1 \qquad \sum_{q=1}^{n}\alpha_q = 1 \tag{5}$$

In order to visualize the turbulent phenomenon in a flow, a specific mathematical treatment is required, which should be selected in accord to the desired accuracy in the numerical simulation and the computational power available. Therefore, a simplified approach to turbulence is achieved through the RANS models. The RANS models are originated from the average processes on Navier-Stokes equations [11], among the available RANS models the SST $\kappa - \omega$ [20] stands out, given its wide applicability in engineering issues, which is justified by its great ability to describe the zones near walls [12].

$$\rho \overline{u_j}\frac{\partial k}{\partial x_j} = \frac{\partial}{\partial x_i}\left[\left(\mu + \frac{\mu_T}{\sigma_\varepsilon}\right)\frac{\partial k}{\partial x_i}\right] + \rho P_k - \rho\varepsilon \tag{6}$$

$$\frac{\partial(\rho\omega)}{\partial t} + div(\rho\omega U) = div\left[\left(\mu + \frac{\mu_\tau}{\sigma_{\omega,1}}\right)grad(\omega)\right]$$
$$+\gamma_2\left(2\rho S_{ij}.S_{ij} - \frac{2}{3}\rho\omega\frac{\partial U_i}{\partial x_j}\delta_{ij}\right) - \beta\rho\omega^2 + 2\frac{\rho}{\sigma_{\omega,2}\omega}\frac{\partial \kappa}{\partial x_\kappa}\frac{\partial \omega}{\partial x_\kappa} \tag{7}$$

The equations 6 and 7 constitute a model, in which κ represents the turbulent kinetic energy generated and ω represents the specific dissipation rate, while written in index notation, there is i, j, k which represents the spatial directions, k the turbulent kinetic energy, ω the turbulent frequency and U the average flow velocity. The fine adjustment of the model in question is attained by the calibration of the value of the constants σ_κ, $\sigma_{\omega,1}$, $\sigma_{\omega,2}$, γ_2, β_2 e $\beta*$ according to the correlated literature [21].

3 Methodology and Validation

A 2D geometry with dimensions shown in Figure 1 was used as a domain for the simulations. To ensure the accuracy of the results, four tetrahedral meshes with distinct element sizes were created. For all four models, the air injection occurs from the inferior area of the geometry at 0.1 m/s, with atmospheric pressure at the exit and water level at 400 mm at the initial time. The multiphase flow in question is considered incompressible and was processed using the commercial software ANSYS Fluent, that in turn uses a finite volume algorithm. For the simulation an Intel Core i7 and 16GB of RAM DDR4 were employed.

Given the turbulent nature of the flow, the selected convergence criteria for the mesh test was based on y^+. This parameter has by definition a wall shear tension, which numerically varies as a result of the mesh resolution, whose value should be in the order of $y^+ < 5$ in the viscous sublayer, in a different situation the mesh should be remodeled [22]. On Table 1 it's possible to observe the convergence of the meshes 3 and 4, considering that they meet the previously mentioned criteria and possess values within a close range. The mesh 3 was chosen to perform the simulations, since it has circa of 40% less nodal points, which reduces the required computational processing of the simulation while still maintaining the satisfactory results.

Figure 1. Geometry.

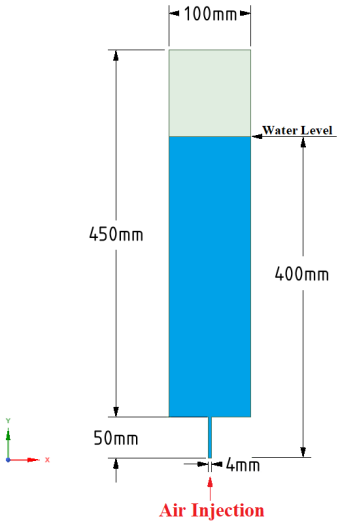

Table 1. Mesh Results.

Mesh	Element size	Nodes	y^+
1	6	11848	12.78
2	4	22405	8.43
3	2	97453	3.77
4	1.5	169666	3.22

The simulations in transient regimes were performed using the volume of fluid (VOF) multiphase model with an explicit scheme, the $SST\ \kappa-\omega$ turbulence model, implicit model of body force and two Eulerian phases, which were defined as primary and secondary, according to the data presented in Table 2. This multiphase model does not make use of an specific differential equation to treat the interface, therefore tracking the interface positioning through volumetric fraction maping. The chosen surface tension force model was the continuum surface force (CSF) includes an adequate interface curvature treatment and a specific expression for the bubble-liquid interface force, as seen in detail in [23], [19].

Table 2. Properties of the liquid phase and gaseous phase used in the simulation.

$\rho_{air}{}^{(kg/m^3)}$	$\rho_{water}{}^{(kg/m^3)}$	$\mu_{air}{}^{(Pas)}$	$\mu_{water}{}^{(Pas)}$
1.225	998.2	1.7894e-5	0.001

Source: Author.

The validation of the achieved results with mesh 3 were based on the works of Liu [23], which brings a comparison between his numerical simulations and experimental data obtained from Deen [24], such as shown on

Figure 2a. Once a good agreement between the numerical and empirical data from the authors was established, the simulations using similar geometry generated in this work, as seen on Figure 2b, were compared to those of Liu [23]. Such comparison of the axial velocity profile was made using a tension of $\sigma_s = 0.072$ and velocity of injection of 0.12 m/s, in the axial position of $y = 250mm$. At last, it's possible to observe good adherence between the profiles displayed in Figures 2a and 2b, which allows for an implication on the trustworthiness of the simulations.

Figure 2. Comparison between the works of Liu and Deen against the performed simulation.

(a) Liu's and Deen's work.

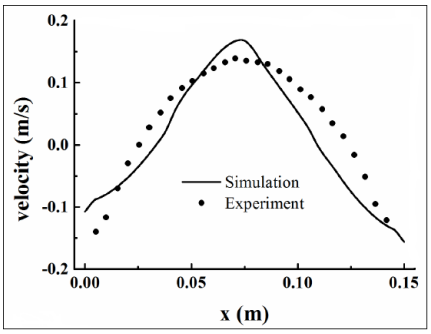

Source: [25]

(b) Performed Simulation.

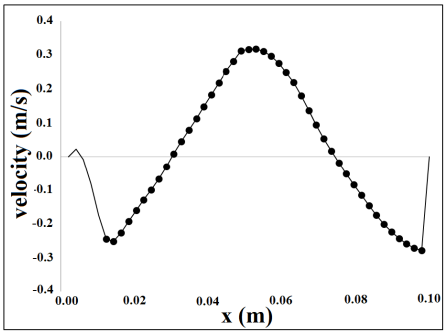

Source: Author.

The parametric analysis of the surface tension in the flow is based on five simulations, in which the properties of the continuous phase are preserved, whilst the surface tension is altered as exhibited on Table 3. Such values are established by adding multiples of the deviation $\Delta\sigma$ to the original σ_s value, which refers to the surface tension of water at 25ºC.

Table 3. Tested values $\sigma_s \pm \Delta\sigma$ with $\Delta\sigma = 0,010N/m$

$\sigma_s - 4\Delta\sigma$	$\sigma_s - \Delta\sigma$	σ_s	$\sigma_s + \Delta\sigma$	$\sigma_s + 4\Delta\sigma$
0.032	0.062	0.072	0.082	0.112

Source: Author.

For the purpose of attaining a qualitative analysis of the results using frames of the flow, the volumetric fraction of the phases was projected in the post-processing of the simulation, where the blue color represents the liquid phase and the red represents the gas phase, whereas the remaining colors represent the interface between the phases.

4 Results and Discussions

The figure 3 below represents the flow with $\sigma_s = 0,072$ at the instant in which the air becomes in contact with water, in the frame $t = 0,4s$ until the first bubble emerges from the liquid, at the instant $t = 2,3s$, which finalizes the analysis. The evaluated frames which constitute the results in Figures 3, 4, and 5 correspond, from left to right, to the instants brought by table 4.

Table 4. Instant of times analized in the numerical simulations

Frame 1	Frame 2	Frame 3	Frame 4	Frame 5	Frame 6	Frame 7	Frame 8
0.4	0.6	1.0	1.2	1.5	1.8	2.0	2.3

Source: Author.

The comparison between Figures 3, 4a and 4b reveals a slight change in the presented flows. Moreover, it's noted that, in the same time frame, in the topologies with a smaller surface tensions, the bubbles display great lateral movement, while in cases with higher surface tension, the bubbles tend to remain close to the center of the geometry. It's feasible to visually assert that the mechanism of bubble breaking was little affected by this slight change in the original values of flow tension. In a preliminary manner, it's possible to infer that the smaller values

Figure 3. Flow with $\sigma_s = 0.072$.

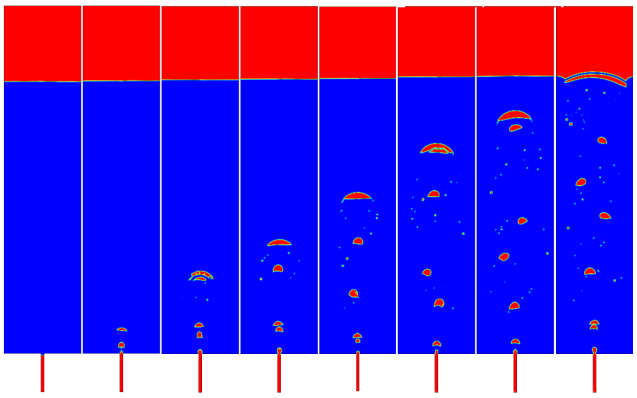

Figure 4. Flow with $\sigma_s \pm \Delta\sigma$

(a) $\sigma_s - \Delta\sigma(0.062N/m)$ (b) $\sigma_s + \Delta\sigma(0.082N/m)$

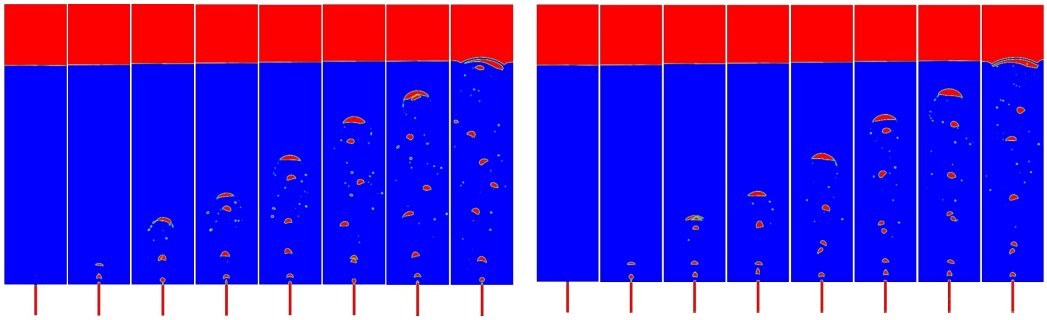

of surface tension seem to allow the disperse phase to become more susceptible to a zigzag movement [26] in less time, nevertheless, this behavior has an inflexion as displayed in Figure 5a.

The influence of surface tension in breaking and coalescence of bubbles is more evident in Figures 5, where a lower tension between the phases cause certain instability in the structure of the bubbles, which break in smaller ones more easily [27]. The centralized path pattern of the bubbles in Figure 5b shows, again, a greater perturbation inertia in the flow on this level of tension. It's concluded that the point of inflexion, cited at the analysis of the Figure 4, refers to the magnitude of the tension value, in which a possible inertial advantage set to the helical movement gives place to an intense break mechanism, that is amplified by a lesser cohesion of the disperse phase.

Figure 5. Flow with $\sigma_s \pm 4\Delta\sigma$

(a) $\sigma_s - 4\Delta\sigma(0.032N/m)$ (b) $\sigma_s + 4\Delta\sigma(0.112N/m)$

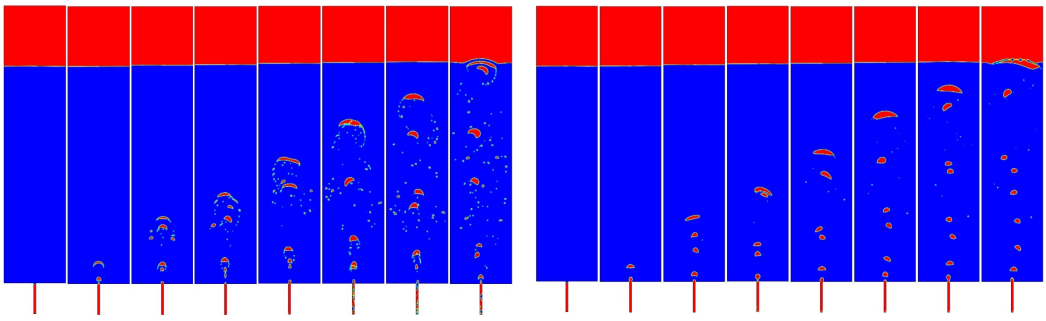

The last analysis, performed on Figure 6, consists of opposing simulations with the levels of surface tensions displayed in Table 3 for two total times of transient simulation. Firstly, it's noted that the smaller levels of tension magnitude present greater changes between two temporal frames and, therefore, they are not close to the permanent regime. In a complementary manner, in relation to the greater tension levels, there already was a tendency in helical path or zigzag in the simulation with $t = 3.5s$, which is confirmed in a more sinuous and evident manner in the simulation with $t = 5.0s$, that varies little in time, especially in the last level of surface tension.

Figure 6. Comparison of simulations with total time of $t = 3.5s$ and $t = 5.0s$

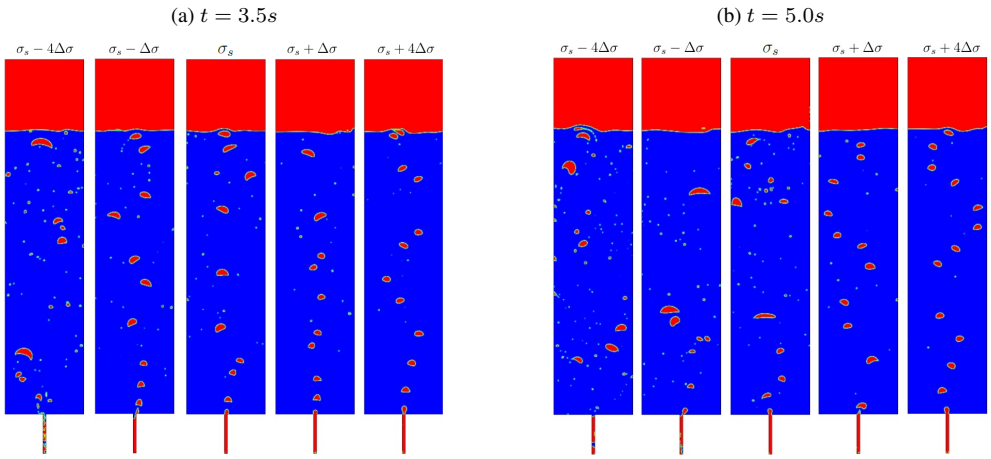

5 Conclusions

In regards to the numerical approach of multiphase flow, the selection of the multiphase model as well as the modelling of the turbulence are interdependent, that is, both must be adjusted in order to provide with a trustworthy description of the phenomena and its correlate conditions. The combination of the VOF model with the turbulent treatment via SST $\kappa - \omega$ has proven to be efficient in the proposed case study, since the curves of the axial velocity align in a satisfactory manner with the numerical results and experimental data available in the literature.

The results generated by the parametric analysis reveal a clear dependency between the mechanisms of breaking and coalescence and the magnitude of surface tension. The analysis method, given by the examination of a sequence of instants of time, has proven to be efficient in revealing the topology of the phases as well as its special variation. Two concurrent effects were identified, which arise in an eventual decrease in tension: the reduction of inertia in the disperse phase, that leads to movement in zigzag in less time versus a tendency in the increase of the break mechanism. For greater levels of superficial tension, there is a natural strengthening in the mechanism of coalescence, which makes the stationary regime seem to be achieved in less time.

The evidence raised by the qualitative analysis of the surface tension magnitude demands further studies via numerical quantitative investigation and experimental approaches. The preliminary exposure of the results displayed is part of a line of research, which is structured in the investigation of the mechanisms of break up and coalescence, as well as assessing its sensitivity to various physical-mathematical parameters such as the flow rate of the injection of the dispersed phase, spatial position of the injection and also the selection of constitutive models of relevant interfacial forces, such as drag, surface tension forces, lift forces, wall forces, among many others. Thus, there is a demand in extending the research towards the aforementioned parameters, in order to enhance the fundamental understanding on the dynamics of the mechanisms of breaking and coalescence of bubbles.

5.1 Authorship Statement

The authors hereby confirm that they are the sole liable persons responsible for the authorship of this work, and that all material that has been herein included as part of the present paper is either the property (and authorship) of the authors, or has the permission of the owners to be included here.

References

[1] Rosa, E. S., 2009. *Escoamento multifásico isotérmico: modelos de multifluidos e de mistura*. Bookman.
[2] Brennen, C. E., 2005. *Fundamentals of multiphase flow*. Cambridge university press.
[3] Cely, M. M. H., Baptistella, V. E., & Rodriguez, O. M., 2018. Study and characterization of gas-liquid slug flow in an annular duct, using high speed video camera, wire-mesh sensor and piv. *Experimental Thermal and Fluid Science*, vol. 98, pp. 563–575.
[4] Prosperetti, A. & Tryggvason, G., 2009. *Computational methods for multiphase flow*. Cambridge university press.
[5] Chen, Z., Huan, G., & Ma, Y., 2006. *Computational methods for multiphase flows in porous media*. SIAM.
[6] Ishii, M. & Hibiki, T., 2010. *Thermo-fluid dynamics of two-phase flow*. Springer Science & Business Media.
[7] Yamoah, S., Martínez-Cuenca, R., Monrós, G., Chiva, S., & Macián-Juan, R., 2015. Numerical investigation of models for drag, lift, wall lubrication and turbulent dispersion forces for the simulation of gas–liquid two-phase flow. *Chemical Engineering Research and Design*, vol. 98, pp. 17–35.
[8] Ziegenhein, T., Tomiyama, A., & Lucas, D., 2018. A new measuring concept to determine the lift force for distorted bubbles in low morton number system: Results for air/water. *International Journal of Multiphase Flow*, vol. 108, pp. 11–24.
[9] Hirt, C. & Nichols, B., 1981a. Volume of fluid (vof) method for the dynamics of free boundaries. *Journal of Computational Physics*, vol. 39, n. 1, pp. 201–225.
[10] Michaelides, E., Crowe, C. T., & Schwarzkopf, J. D., 2016. *Multiphase flow handbook*. CRC Press.
[11] Pope, S. B., 2000. *Turbulent flows*. Cambridge University Press.
[12] Versteeg, H. K. & Malalasekera, W., 2007. *An introduction to computational fluid dynamics: the finite volume method*. Pearson Education.
[13] Tennekes, H., Lumley, J. L., Lumley, J. L., et al., 1972. *A first course in turbulence*. MIT press.
[14] Corson, D., Jaiman, R., & Shakib, F., 2009. Industrial application of rans modelling: capabilities and needs. *International journal of Computational Fluid dynamics*, vol. 23, n. 4, pp. 337–347.
[15] Faria, C. L., 2017. Simulação numérica do escoamento multifásico água-ar induzido pela injeção de ar pelo fundo de um reator. *Universidade Federal do Espírito Santo, Vitória*.
[16] Reddy, J., 2010. *Principles of continuum mechanics*. Cambridge University Press Cambridge.
[17] Slattery, J. C., 1999. *Advanced transport phenomena*. Cambridge University Press.
[18] Hirt, C. W. & Nichols, B. D., 1981b. Volume of fluid (vof) method for the dynamics of free boundaries. *Journal of computational physics*, vol. 39, n. 1, pp. 201–225.
[19] ANSYS, F., 2013. Ansys fluent theory guide. *ANSYS Inc*.
[20] Menter, F. R., 1994. Two-equation eddy-viscosity turbulence models for engineering applications. *AIAA journal*, vol. 32, n. 8, pp. 1598–1605.
[21] Wilcox, D. C. et al., 1998. *Turbulence modeling for CFD*, volume 2. DCW industries La Canada, CA.
[22] ANSYS, F., 2015. Ansys fluent manual: Multiphase modeling using.
[23] Liu, Q. & Luo, Z., 2019a. Modeling bubble column reactor with the volume of fluid approach: Comparison of surface tension models. *Chinese Journal of Chemical Engineering*, vol. 27, n. 11, pp. 2659–2665.
[24] Deen, N. G., Solberg, T., & Hjertager, B. H., 2001. Large eddy simulation of the gas–liquid flow in a square cross-sectioned bubble column. *Chemical engineering science*, vol. 56, n. 21-22, pp. 6341–6349.
[25] Liu, Q. & Luo, Z., 2019b. Modeling bubble column reactor with the volume of fluid approach: Comparison of surface tension models. *Chinese Journal of Chemical Engineering*.
[26] Chen, C. & Fan, L.-S., 2004. Discrete simulation of gas-liquid bubble columns and gas-liquid-solid fluidized beds. *AIChE Journal*, vol. 50, n. 2, pp. 288–301.
[27] Yan, P., Jin, H., He, G., Guo, X., Ma, L., Yang, S., & Zhang, R., 2020. Numerical simulation of bubble characteristics in bubble columns with different liquid viscosities and surface tensions using a cfd-pbm coupled model. *Chemical Engineering Research and Design*, vol. 154, pp. 47–59.